Role of heat dissipation in polarization switching of ferroelectrics

Haohua Wen,[1,2,3,4] Jianyi Liu,[5,1,2,3] Weijin Chen,[1,2,3,6] and Yue Zheng[1,2,3,*]
[1] *Guangdong Provincial Key Laboratory of Magnetoelectric Physics and Devices, School of Physics, Sun Yat-sen University, Guangzhou 510275, China*
[2] *State Key Laboratory of Optoelectronic Materials and Technologies, School of Physics, Sun Yat-sen University, Guangzhou 510275, China*
[3] *Centre for Physical Mechanics and Biophysics, School of Physics, Sun Yat-sen University, Guangzhou 510275, China*
[4] *Sino-French Institute of Nuclear Engineering and Technology, Sun Yat-sen University, Zhuhai 519082, China*
[5] *College of Physics, Qingdao University, Qingdao 266071, China*
[6] *School of Materials, Sun Yat-sen University, Shenzhen 518107, China*

(Received 28 April 2023; revised 28 August 2023; accepted 28 September 2023; published 23 October 2023)

Polarization switching in ferroelectrics by applying external fields is a typical thermodynamic process. Heat dissipation plays an inevitable role, especially in ultrafast and nonequilibrium switching processes. Its role has long been neglected in existing theoretical models focusing on conservative actions. In this paper, a dynamic phase diagram is derived to consider the heat dissipation on equal footing with the work done by external field. Their competition leads to four switching mechanisms. The dynamic and thermodynamic analyses are then performed to verify the inevitable mechanisms dominated by heat dissipation. Our finding refreshes the understanding of polarization dynamics.

DOI: 10.1103/PhysRevB.108.134114

I. INTRODUCTION

External field-driven polarization switching is a key issue in the fundamental physics and functional device applications for ferroelectrics [1–6]. As a typical thermodynamic process for polarization switching, besides work done by external field, heat dissipation also dominates the polarization microstructural evolution [7], especially in the strong nonequilibrium ultrafast process [8]. Several theoretical models are proposed to describe the polarization switching mechanism, which can explain most experimental results [9], such as Merz's law [10], Kolmogorov-Avrami-Ishibashi [11], nucleation-limited switching (NLS) [12], and homogeneous switching [13] models. Unfortunately, most of them focus on the conservative action of external field, but do not consider the heat dissipation action on equal footing [14,15]. Hence, the disparity is usually found between the experimental measurement and the theoretical prediction [16]. In addition, since the applicable conditions and criteria among different models are not well-addressed, it brings confusion to the mechanistic understanding of polarization switching under different conditions [17]. To solve this problem, a comprehensive understanding of the heat dissipation role is a key step [7,8], which is the aim of this paper.

II. ANALYTICAL MODEL

Starting with a simple double-well model, a dynamic phase diagram of polarization switching is derived to address the electric and thermal actions, and the simulations of stochastic phase field model (SPFM) [18] are performed to demonstrate the physical picture. To simplify the discussion without losing generality, we consider the polarization switching process in a perfect $BaTiO_3$ (BTO) crystal with monodomain driven by a reverse electric field E. BTO is a typical ferroelectric, having spontaneous polarization of $P = \lambda \approx 0.26\,\mathrm{C/m^2}$ at $T = 300\,\mathrm{K}$. Following the Landau-Ginzburg-Devonshire (LGD) theory [19], the polarization dynamics in BTO under a reverse electric field E at a fixed temperature of $T = 300\,\mathrm{K}$ can be described by a double-well form free-energy landscape $F = F(P, E)$ with the polarization P_z as the reaction coordinate. In generally, F can be simply expressed as

$$F = F(P, E) = \frac{\Omega}{8\varepsilon\lambda^2}[(P^2 - \lambda^2)^2 - \lambda^4] - \Omega EP. \quad (1)$$

Here, Ω is the volume occupied by the polar element, and ε is the effective dielectric constant. The black line in Fig. 1(a) shows the free-energy profile in the case of $E = 0$, where the ferroelectric system of BTO has two symmetrical steady states as $P_m^{\pm} = \pm\lambda$ (P_m means the states with local or global free energy minimum), separated by a saddle-point state of $P_s = 0$. Therefore, it requires enough energy to overcome the barrier of $F_B = F(P_s) - F(P_m)$ for the phase transition between two steady states $P_m = \pm\lambda$, i.e., the polarization switching. Applying an electric field E will bias F and change $P_m = P_m(E)$. In particular, there is a critical electric field $E_C = \sqrt{3}\lambda/9\varepsilon$ as shown in Fig. 1(a). If a strong field is applied as $E > E_C$, we can get $F_B < 0$, and there is only one stable state of P_m^+ [see the blue line in Fig. 1(a)]. Therefore, the polarization switching can directly occur from P_0 to P_m^+ without overcoming any barrier. This is the so-called homogeneous switching mechanism reported in literature [i.e., mechanism I with $E > E_C$ in Fig. 1(f)].

---

[*] Corresponding author: zhengy35@mail.sysu.edu.cn

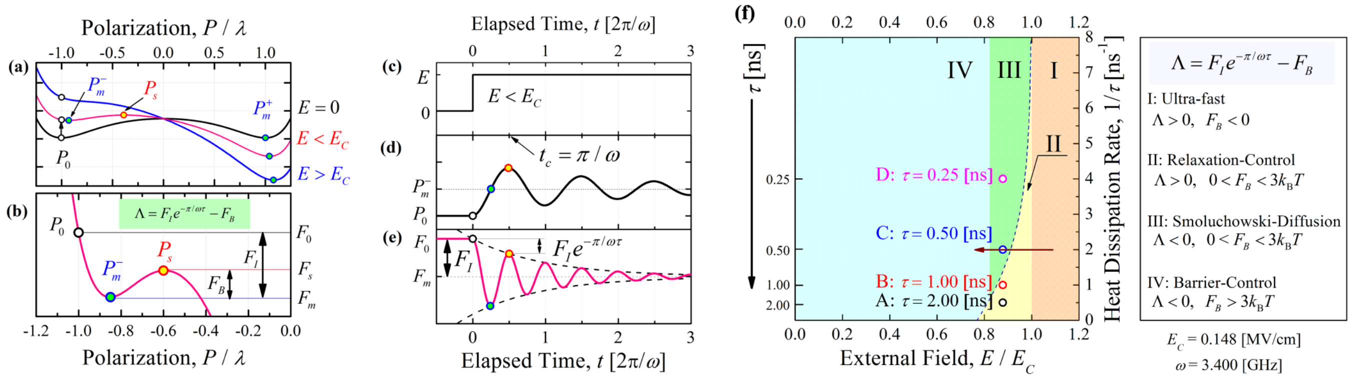

FIG. 1. Schematics for the deduction of dynamic phase diagram of polarization switching and its criterion Λ. (a) The biased free energy profile under the applied positive external field E; (b) the enlarged figure of the free energy profile in the case of $E < E_C$; (c) the setting of applied field; the evolution behaviors of (d) $P = P(t)$ and (e) $F = F(t)$ based on Tani's equation. (f) The dynamic phase diagram of polarization switching with the electric field E/E_C and heat dissipation rate $1/\tau$ as the reaction coordinates.

When $E < E_C$, there are still two steady states named P_m^+ and P_m^-, and a saddle point state of P_s, giving rise to a finite barrier $F_B > 0$ for polarization switching. Assuming $E = 0$ at $t < 0$, the system stays at one symmetric steady state of $P = P_0 = -\lambda$, which needs to cross the saddle-point state of $P_s = 0$ and reach another state of $P = \lambda$ to realize the polarization switching. For a sufficiently large polar element, its thermal fluctuation cannot help overcome F_B [18], i.e., $F_B \gg k_B T$, so polarization switching cannot occur spontaneously. Applying a reverse field E at $t = 0$ will bias F and change the steady-state position as $P_m^- \neq -\lambda$, so the system gets an initial energy of $F_I = F(P_0, E) - F(P_m^-, E)$ for it relaxing from P_0 to P_m^- at $t > 0$ [see Fig. 1(b)], and the transition barrier F_B is also compressed. In this case, the polarization switching is determined by the relaxation evolution of polarization dynamics under the actions of electric field and heat dissipation. Such a relaxation process would occur with time elapsed as $t > 0$, which can be described by Tani's relaxation equation [20], i.e.,

$$\mu \ddot{P} = -\frac{\partial F}{\partial P} - \gamma \dot{P}, \quad \text{as} \quad P(t = 0) = P_0, \tag{2}$$

where μ is the effective mass and γ is the friction coefficient. $-\frac{\partial F}{\partial P}$ and $-\gamma \dot{P}$ are, respectively, the conservative and dissipative forces acting on the polarization. Under these two actions, $P(t)$ reveals the decayed oscillation around its stable state of P_m^- starting from P_0, as [see Fig. 1(d)]

$$P(t) = P_m^- + (P_0 - P_m^-)e^{-t/2\tau}\cos(\omega t), \tag{3}$$

where ω is the vibrational frequency of polarization near P_m^-, as

$$\omega^2 = \omega_0^2 - \frac{\gamma^2}{4\mu^2}, \quad \text{as} \quad \omega_0^2 = \frac{1}{\mu}\left.\frac{\partial^2 F}{\partial P^2}\right|_{P_m^-}, \tag{4}$$

and τ is the characteristic relaxation time of polarization. Its value is determined by the dissipative coefficient of γ, for instance, $\tau = \mu/\gamma$ in the case of decayed oscillation described by Eq. (2) (readers can see detailed discussion in Ref. [8]). Correspondingly, the evolution of free energy $F(t) = F(P(t))$ can be derived as [8,18]

$$F(t) = F_m + F_I e^{-t/\tau}\cos(2\omega t), \tag{5}$$

which is shown in Fig. 1(e). In this decayed oscillation (relaxation) process, the moment for the first attempt to go over the saddle-point state of P_s reads $t_c = \pi/\omega$. If $F(t = t_c) > F_s$, the system can overcome the P_s state and directly relax to the reverse state of P_m^+ to finish the polarization switching. Otherwise [if $F(t = t_c) < F_s$], it will continue the relaxation process, and stay at $P = P_m^-$ with thermal fluctuations. Therefore, we can define a criterion Λ to describe these two polarization switching mechanisms, as

$$\Lambda = F_I e^{-t_c/\tau} - F_B = F_I e^{-\pi/\omega\tau} - F_B, \tag{6}$$

where F_I is the initial energy for the polarization relaxation and F_B is the energy barrier for the polarization switching [see the physical picture in Fig. 1(b)]. In particular, we have

$$\begin{aligned} \Lambda > 0 \quad &\Leftrightarrow \quad F(t_c) > F_s \\ \Lambda < 0 \quad &\Leftrightarrow \quad F(t_c) < F_s. \end{aligned} \tag{7}$$

It should be emphasized that, given the same initial state of $P = P_0$ and the applied $E < E_C$, the value of Λ in Eq. (6) will be determined by the heat dissipation rate characterized by $1/\tau$ to affect the polarization switching. For a proper electric field applied $E < E_C$ that makes $F_I > F_B$ [e.g., see the energy profile illustrated in Fig. 1(b)], a slow heat dissipation rate during the polarization relaxation would result in $\Lambda > 0$, i.e., $F(t_c) > F_s$, which means that the system will have enough energy to go over the switching barrier in the first decayed oscillated period. In this case, although the applied electric field is weaker than the thermodynamic coercive field as $E < E_C$, the system has the chance to achieve the polarization switching in a very short time, which has the same magnitude of the characteristic vibration time as $t_S \sim t_c = \pi/\omega \sim 1$ ns. This is mechanism II of the phase diagram in Fig. 1(f). Otherwise, if the heat dissipation rate is sufficient large to result in $\Lambda < 0$ (i.e., $F(t_c) < F_s$, which means that the system loses too much energy due to the heat dissipation), the system cannot go through P_s and will turn back to P_m^- with thermal fluctuations. According to Kramers' theory [21], it would gain enough energy to go over the barrier F_B under the thermal assistance with time elapsed. This is the physical essence of the NLS mechanism. The occurrence of polarization switching is determined by the competition between the energy barrier F_B and thermal fluctuation $k_\mathrm{B}T$. It has been demonstrated in various diffusion phenomena that, in the cases of $F_B < 3k_\mathrm{B}T$, the system will undergo the Brownian motion under a finite potential well, which is called Smoluchowski-diffusion [22], so the polarization switching can occur in a short time, that t_s ranges from several nanoseconds to microseconds, corresponding to mechanism III of the phase diagram in Fig. 1(f). In contrast, if $F_B > 3k_\mathrm{B}T$ due to a weak electric field E applied, the polarization switching process would be of the quasiequilibrium one, that t_S will reach the order of milliseconds or seconds, corresponding to mechanism IV of the phase diagram in Fig. 1(f).

With the actions of applied electric field and heat dissipation, i.e., the conservative and dissipative forces, we can get four kinds of polarization switching mechanisms. Defining E/E_C and $1/\tau = \gamma/\mu$, respectively, representing the intensities of the electric and thermal forces, a dynamic phase diagram can be obtained [see Fig. 1(f)]. Note that heat dissipation plays the dominant role in the cases that $E \lesssim E_C$, resulting in the (II) relaxation-controlled and (III) Smoluchowski-diffusion mechanisms, which is not well-addressed in literature. In this following, we will perform SPFM simulations of polarization dynamics to demonstrate the mechanisms shown in the dynamic phase diagram.

In SPFM [18], the BTO bulk is treated as an ensemble of N polar elements (grids) embedded into a Langevin heat bath denoted by $T = 300\,\mathrm{K}$. Using P_i as the degree of freedom ($P_i = P_{n,\alpha}$ represents the α component of the nth grid polarization with $n = 1, 2, \ldots, N$ and $\alpha = x, y, z$), the many-body Hamiltonian $\mathcal{H}$ reads [18]

$$\mathcal{H} = \mathcal{K} + \mathcal{U} + \mathcal{H}_E + \mathcal{H}_\mathrm{HB}. \tag{8}$$

Here, $\mathcal{K} = \sum_i \frac{1}{2}\mu\dot{P}_i^2$ is the kinetic energy. $\mathcal{U}$ is the LGD interaction (see details in the Appendix). $\mathcal{H}_E = -\sum_i \Omega E P_i$ is the electrostatic potential. $\mathcal{H}_\mathrm{HB}$ denotes the actions of heat bath, including the dissipation $-\gamma\dot{P}_i$ and fluctuation $\xi_i(t)$. The Langevin equation is thus derived as [18]

$$\mu\ddot{P}_i = -\frac{\partial\mathcal{F}}{\partial P_i} - \gamma\dot{P}_i + \xi_i(t). \tag{9}$$

Here, $\mathcal{F} = \mathcal{U} + \mathcal{H}_E$ describes the conservative actions [23] and $\xi_i(t)$ is the Gaussian random force as $\langle\xi_i(t)\rangle = 0$ and $\langle\xi_i(t)\xi_j(t')\rangle = 2\gamma k_\mathrm{B}T\delta_{ij}\delta(t-t')$. The system is set as an infinite BTO bulk of $N = 64^3$ grids with grid size as $\Omega = 64\,\mathrm{nm}^3$ to let the LGD energy be compatible with the thermal fluctuations [18].

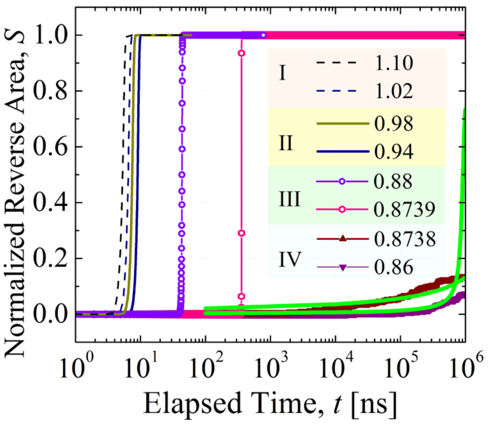

FIG. 2. The simulation results of polarization switching [characterized by the time dependence of the normalized reverse area $S(t)$ of Eq. (10)] along the blue arrow in Fig. 1(f) based on SPFM with a fixed $\tau = 0.50\,\mathrm{ns}$ and various E applied, which covers the four mechanisms.

Fixing $\tau = 0.50\,\mathrm{ns}$, Fig. 2 plots the SPFM simulation results under various E covering those four mechanisms in Fig. 1(f), where the time-dependent normalized reverse area $S(t)$ is used to described the polarization switching process [15]. (I) Ultrafast switching mechanism, where the energy barrier disappeared, i.e., $F_B < 0$, due to the applied strong electric field as $E > E_C$, and each grid can thus reverse ultrafast without crossing any barrier, e.g., $t_S \sim 5\,\mathrm{ns}$ under $E/E_C = 1.10$ and 1.02 shown in Fig. 2. Here t_S is the switching time, i.e., the time interval for the system evolving from $P = P_0$ to $P = 0$. (II) Relaxation-controlled mechanism. With $E \lesssim E_C$, there is a finite barrier $F_B > 0$, and the system will relax from P_0 to P_m^- at first. Although there is heat dissipation, because a large E applied ensures $\Lambda > 0$, it can still have enough energy as to cross P_s during the first relaxation cycle and get a rapid polarization switching, e.g., $t_S \sim 10\,\mathrm{ns}$ under $E/E_C = 0.98$ and 0.94 shown in Fig. 2, having the same order of magnitude with that of (I). (III) Smoluchowski-diffusion mechanism. A weaker E-field applied makes $\Lambda < 0$, the system thus loses too much energy during relaxation. It fails to cross P_s and keeps metastable at P_m^- with thermal fluctuation. Since $F_B < 3k_\mathrm{B}T$, the system carries on the Brownian motion upon a potential surface, i.e., Smoluchowski diffusion [22] in phase space, so polarization switching occurs in a short time [21], e.g., $10\,\mathrm{ns} < t_S < 10^3\,\mathrm{ns}$ under $E/E_C = 0.88$ and 0.8739 plotted in Fig. 2. (IV) Barrier-controlled mechanism. Since E/E_C is so small that $F_B \gg k_\mathrm{B}T$, reversals of minor polar-elements are observed within $t = 10^6\,\mathrm{ns}$ shown in Fig. 2. This is a quasiequilibrium process, having a similar physical picture with NLS mechanism [12], e.g., $S(t)$ under $E/E_C = 0.8738$ and 0.86 is found to be well described by Tagantsev's formula [15,24], i.e.,

$$S(t) = \frac{1}{2} + \frac{1}{\pi}\mathrm{atan}\left(\frac{\ln(t) - \ln(\bar{t}_S)}{\ln(w)}\right). \tag{10}$$

Here, $\bar{t}_S$ and w are the mean switching time and its variance, respectively. As plotted in the green lines in Fig. 2, we can get $\bar{t}_S = 0.40 \times 10^6\,\mathrm{ns}$ and $w = 1.30\,\mathrm{ns}$ for the case of $E/E_C = 0.8738$, and $\bar{t}_S = 1.67 \times 10^6\,\mathrm{ns}$ and $w = 1.15\,\mathrm{ns}$ for the case of $E/E_C = 0.86$, respectively. In addition, a shape boundary is found between (III) and (IV) mechanisms, that decreasing E/E_C from 0.8739 to 0.8738 makes t_S rapidly increase from 10^2 to 10^6 ns. It is probably caused by underestimating the polar-element-interaction in LGD theory [19], leading to the weak dynamical correlations. Hence, each polar element mainly gains energy from its thermal fluctuation, not the interaction provided by its neighbors.

Note that the phase diagram of Fig. 1(f) is not a precise one since the thermal action is overestimated based on Tani's equation [20]. We thus modify $\omega = 3.4\,\mathrm{GHz}$ in Λ to correct it to meet the SPFM simulation results. In addition, the steep rising edge of E applied is different from the common experimental setting. However, the phase diagram has a general validity for polarization switching, where the roles of electric

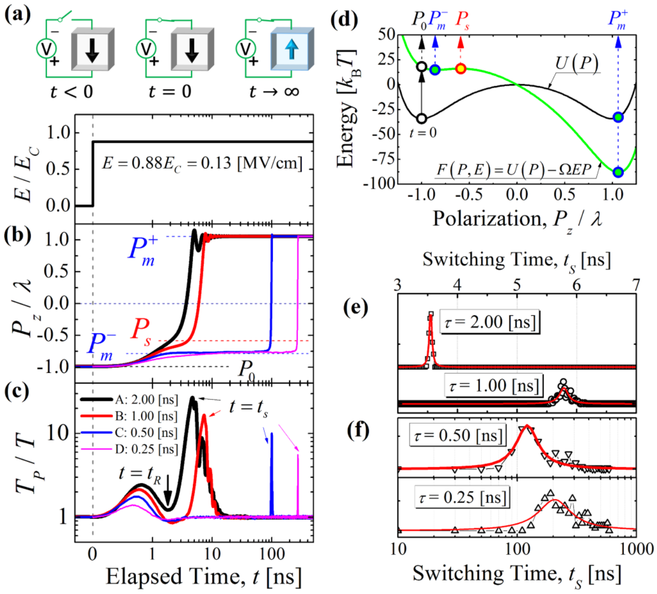

FIG. 3. The dynamic description of polarization switching process. (a) The setting and (d) the energy profile of the polarization switching process studied; (b) the polarization and (c) its temperature evolution; (e), (f) the stochastic distribution of switching time t_S observed.

and thermal forces are well-addressed. According to Λ of Eq. (6), the E field determines F_I and F_B, and heat dissipation effect is reflected in the factor $e^{-\pi/\omega\tau}$, directly determining the dynamical behavior, especially the presence of (II) and (III) polarization-switching mechanisms. Most theoretical models focus on the conservative action but do not fully consider the role of heat dissipation [7,25,26]. The thermodynamic coercive field $E_{\rm th}$ is defined as the minimum E field required to drive the polarization switching [27], e.g., $E_{\rm th} = 0.13$ MV/cm in Fig. 2. Note that $E_{\rm th}$ is usually found in experiments being smaller than the LGD prediction E_C [9], which is also found in our simulations as $E_C = 0.148$ MV/cm. The fact of $E_{\rm th}$ relying on τ and E cannot completely be interpreted by the conservative impacts [28]. Otherwise, Λ is a more physical quantity, involving both conservative and dissipative roles. In a word, polarization switching is a thermodynamic process, where the heat dissipation role cannot be well-described in a conservative way. To further address this conjecture, we will analyze the dynamics and thermodynamics of polarization switching processes and verify the rationality and inevitability of the resulting (II) and (III) mechanisms.

III. DYNAMICAL ANALYSIS

We can discuss the heat dissipation effects based on the simulations with fixing E applied and changing τ. As shown in Fig. 3, the polarization-switching process is simulated under $E/E_C = 0.88$, that $F_I = 3.14k_BT > F_B = 1.29k_BT$ [here, as shown in Fig. 1(b), F_I is the initial energy for the polarization relaxation and F_B is the energy barrier for the polarization switching], with various τ as A: 2.00, B: 1.00, C: 0.50, and D: 0.25 ns. Referring to Fig. 1(f), polarization switching in cases A and B are of (II) the relaxation-controlled mechanism and the ones in cases C and D are of (III) the Smoluchowski-diffusion mechanism. In cases A and B, $\Lambda > 0$ is owed to the small heat dissipation rate, and the system can finish the polarization switching with t_S, respectively, as 3.6 and 5.9 ns in cases A and B. Otherwise, in cases C and D, a large heat dissipation rate leads to $\Lambda < 0$. Since $F_B < 3k_BT$, Smoluchowski diffusion of the system makes polarization switching occur with t_S, respectively, as 100 and 300 ns in cases C and D. As seen from Figs. 3(a)–3(c), there are three subprocesses: (1) field-action sub process of applying E at $t = 0$, (2) relaxation subprocess from P_0 to P_m^- at $0 < t < t_R$ with $t_R \sim 10\pi/\omega$, and (3) reverse subprocess at $t_R < t < t_S$ for the system approaching P_m^+. Since subprocess (1) completes instantaneously, no polarization response and temperature T_P change are revealed (here, $T_P(t)$ is given by $k_BT_P = \langle \mu \dot{P}_i^2 \rangle$). At $t > 0$, T_P rises significantly. Its two peaks correspond to subprocesses (2) and (3), respectively, and the amplitudes of peaks enhance as increasing the heat dissipation rate (with smaller τ). Given the same initial state, the thermal force denoted by τ does not affect the final state that the system reaches, but the evolution process and observed t_S. Note that the observed t_S is stochastic for each individual simulation. Plotted in Figs. 3(e) and 3(f), t_S of cases A and B show the linear Lorentzian distributions, but t_S of cases C and D exhibit the logarithmic ones, which tells again that the presence of (II) and (III) mechanisms is owed to the heat dissipation role [15,24]. In Fig. 3(e), for the cases of relaxation-controlled polarization switching with $\tau = 2.00$ ns and 1.00 ns, t_S satisfies the linear Lorentzian distribution [15,24] as

$$g_1(t_S) = \frac{C}{(t_S - \bar{t}_S)^2 + w^2}. \tag{11}$$

Here, $\bar{t}_S$ and w are the mean switching time and its variance, respectively, and C is a constant. By fitting the SPFM simulations results in accord with Eq. (11), we have $\bar{t}_S = 3.55$ ns and $w = 0.024$ ns for the case of $\tau = 2.00$ ns, and $\bar{t}_S = 5.79$ ns and $w = 0.088$ ns for the case of $\tau = 1.00$ ns, respectively. Otherwise, in Fig. 3(f), for the cases of Smoluchowski-diffusion polarization switching with $\tau = 0.50$ ns and 0.25 ns, t_S satisfies the logarithmic Lorentzian distribution [15,24] as

$$g_2(t_S) = \frac{C}{[\ln(t_S) - \ln(\bar{t}_S)]^2 + [\ln(w)]^2}. \tag{12}$$

After the similar fitting procedure, we can get $\bar{t}_S = 121.5$ ns and $w = 1.29$ ns for the case of $\tau = 0.50$ ns, and $\bar{t}_S = 203.6$ ns and $w = 1.46$ ns for the case of $\tau = 0.25$ ns, respectively.

Although the simulations and resulting polarization-switching mechanisms are obtained based on a specific BTO system and SPFM method, the heat dissipation role revealed is an inevitable thermodynamic result. We will demonstrate the simulated polarization-switching process satisfies the thermodynamic first law, and show the universality, rationality, and inevitability of our conjecture.

IV. THERMODYNAMIC ANALYSIS

According to statistical thermodynamics, the evolution of a many-body system governed by the Hamiltonian $\mathcal{H}$ in Eq. (8) is equivalent to the phase point motion $s(t) = \{P_i(t), \dot{P}_i(t)\}$ in a multidimensional phase space [8]. Considering a process that the system moves from s_0 at t_0 to s_1 at $t_0 + \mathrm{d}t$, the increment $\mathrm{d}A$ of an arbitrary quantity $A = \langle A[s(t)]\rangle$ reads

$$\mathrm{d}A = \langle A[s(t)]\rangle_{s_0}^{s_1} = \langle \dot{A}\,\mathrm{d}t'\rangle_{t_0}^{t_0+\mathrm{d}t} = \langle \dot{A}\,\mathrm{d}t\rangle. \qquad (13)$$

We can then define the internal energy increment $\mathrm{d}U$ as

$$\mathrm{d}U = \langle \mathcal{K} + \mathcal{U}\rangle_{s_0}^{s_1} = \langle \dot{P}_i \cdot (\mu \ddot{P}_i + \partial_i \mathcal{U})\mathrm{d}t\rangle \qquad (14)$$

and the electrostatic potential increment $\text{đ}W$ as

$$\text{đ}W = -\langle \mathcal{H}_E\rangle_{s_0}^{s_1} \equiv \text{đ}W_E - \text{đ}W_O, \qquad (15)$$

where $\text{đ}W_E = \langle \Omega E \dot{P}_i\,\mathrm{d}t\rangle$ and $\text{đ}W_O = -\langle \Omega P_i \dot{E}\,\mathrm{d}t\rangle$ are, respectively, the increments owed to the work done by E and the change of E itself. Correspondingly, the heat dissipation $\text{đ}Q$ occurring from the system to the heat bath is caused by the inequality of polarization temperature T_P and the one of heat bath T, i.e., $T_P \neq T$. Therefore, we can define $\text{đ}Q$ as

$$\text{đ}Q = k_\mathrm{B}(T_P - T)\frac{\mathrm{d}t}{\tau} = \frac{\gamma}{\mu}k_\mathrm{B}(T_P - T)\mathrm{d}t \qquad (16)$$

in the given process mentioned above. Following the deduction in Ref. [18], we can get

$$\frac{\gamma}{\mu}k_\mathrm{B}(T_P - T) = \langle \dot{P}_i \cdot (\gamma \dot{P}_i - \xi_i)\mathrm{d}t\rangle, \qquad (17)$$

which is expressed in form of the negative *work done* by the thermal force, i.e., the fluctuation $\xi_i(t)$ and dissipation forces $-\gamma \dot{P}_i$ revealed in the stochastic dynamic equation of motion in Eq. (9). Therefore, we can link $\text{đ}Q$ with the increment of $\langle \mathcal{H}_\mathrm{HB}\rangle$, as

$$\text{đ}Q = \langle \mathcal{H}_\mathrm{HB}\rangle_{s_0}^{s_1} = \langle \dot{\mathcal{H}}_\mathrm{HB}\mathrm{d}t\rangle = \langle \dot{P}_i \cdot (\gamma \dot{P}_i - \xi_i)\mathrm{d}t\rangle, \qquad (18)$$

which also meets the essence of Ito's stochastic differential equation [29]. Combining Eqs. (14), (15), and (18), we can get

$$\begin{aligned}\mathrm{d}U - \text{đ}W + \text{đ}Q &= \langle \mathcal{K} + \mathcal{U} + \mathcal{H}_E + \mathcal{H}_\mathrm{HB}\rangle_{s_0}^{s_1} = \langle \mathcal{H}\rangle_{s_0}^{s_1} \\ &= \langle \dot{P}_i \cdot (\mu \ddot{P}_i + \partial_i \mathcal{U} - \Omega E + \gamma \dot{P}_i - \xi_i)\mathrm{d}t\rangle - \Omega \dot{E}\langle P_i\rangle \mathrm{d}t.\end{aligned} \qquad (19)$$

According to Eq. (9), we have

$$\mathrm{d}U - \text{đ}W + \text{đ}Q = \langle \mathcal{H}\rangle_{s_0}^{s_1} = -\Omega \dot{E}\langle P_i\rangle \mathrm{d}t = \text{đ}W_O. \qquad (20)$$

Since $\text{đ}W = \mathrm{d}W_E - \text{đ}W_O$ in Eq. (15), we then get the expression of the thermodynamic first law as

$$\mathrm{d}U + \text{đ}Q = \text{đ}W_E. \qquad (21)$$

It describes the energy change in the polarization system due to the heat dissipation and work done by external fields applied. If defining $F = \langle \mathcal{K} + \mathcal{U} + \mathcal{H}_E\rangle$ to describe the energy of the combined system of polarization dynamics and the source of E, we can get another first law expression:

$$\mathrm{d}F + \text{đ}Q = \text{đ}W_O. \qquad (22)$$

Based on Eqs. (21) and (22), we will analyze the thermodynamics of polarization switching process and demonstrate the first law.

As mentioned above, the system undergoes three subprocesses. In subprocess (1), the system is loaded with $E/E_C = 0.88$ at $t = 0$ without any polarization response and heat dissipation, so $\Delta U_1 = Q_1 = W_{E1} = 0$, satisfying the first law as $\Delta U_1 + Q_1 = W_{E1}$ [see Figs. 4(a)–4(c)]. However, there is an electrostatic energy increment before and after loading E as $\langle \mathcal{H}_E\rangle_{t=0^-}^{t=0^+} = W_O = 52.2k_\mathrm{B}T$. It is caused by the sudden change in E, equivalent to the nonelectrostatic work moving the system from infinity ($E = 0$) to the position of $E \neq 0$. This energy increment is shown in Eq. (22) as $\Delta F_1 = W_O$ [see Fig. 4(d)]. At $t > 0$, the polarization evolves under the action of E, accompanying the changes in energy U, work done W, and heat dissipation Q, all of which reveal different evolution behaviors between the subprocesses of (2) and (3). The relaxation subprocess (2) at $t < t_R$ is nearly quasiequilibrium, so the changes in U, W, and Q are slow. Otherwise, the reverse subprocess (3) at $t > t_R$ is likely nonequilibrium, so the changes in U, W, and Q are more rapid. In the whole polarization switching process from P_0 to P_m^+ at $t > 0$ [including subprocesses (2) and (3)], the energy increment reads $\Delta U_2 = U(P_m^+) - U(P_0) = 1.4k_\mathrm{B}T$, the work done $W_{E2} = 106.9k_\mathrm{B}T$, and heat dissipation $Q_2 = 105.5k_\mathrm{B}T$, so $\Delta U_2 + Q_2 = W_{E2}$, satisfying the first law of Eq. (21). In addition, E is fixed at $t > 0$, so $W_O = 0$, leading to $\Delta F_2 + Q_2 = 0$, which also satisfies the first law of Eq. (22). Moreover, the first law can also well describe the entire process from $t < 0$ to $t \to \infty$, that the system moves from the initial state of $P = P_0$ with $E = 0$ to the final state of $P = P_m^-$ with $E \neq 0$, i.e., $\Delta F + Q = W_O$. To sum up, polarization switching is generally a nonequilibrium thermodynamic process governed by the first law, giving rise to a universal and inevitable fact that the actions of the electric and thermal forces dominate the polarization microstructural evolution on the equal footing.

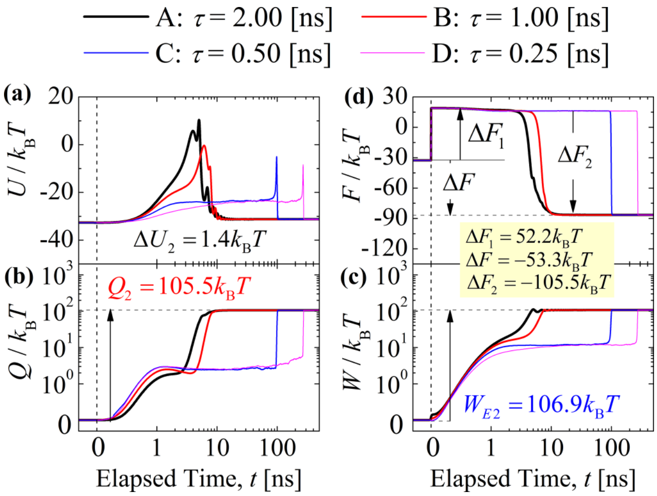

FIG. 4. The thermodynamic description of the same polarization switching process as Fig. 3. The time dependence of (a) internal energy U, (b) heat dissipation Q, (c) work done W, and (d) energy F.

V. CONCLUSION

We studied the inevitable role of heat dissipation in polarization switching of ferroelectrics. A dynamic phase diagram was derived to address the action of heat dissipation on equal footing with the conservative one of external field. The stochastic phase field simulations of polarization switching in $\mathrm{BaTiO_3}$ were then performed to demonstrate the physical picture. The dynamic and thermodynamic analyses were carried out to further address the role of heat dissipation and verify the rationality and inevitability of the resulting (II) and (III) switching mechanisms. Our study refreshes the understanding of polarization dynamics in ferroelectrics.

ACKNOWLEDGMENTS

This study was supported by the National Natural Science Foundation of China (NSFC) (Grants No. 12002400, No. 12132020, and No. 11972382), Guangdong Provincial Key Laboratory of Magnetoelectric Physics and Devices (No. 2022B1212010008), and the Guangdong Basic and Applied Basic Research Foundation (Grant No. 2022A1515010249). The simulations reported were performed on resources provided by the National Supercomputer Center in Guangzhou, the Guangdong Provincial Key Laboratory of Magnetoelectric Physics and Devices (LaMPad) and the Centre for Physical Mechanics and Biophysics (CPMB) in School of Physics in Sun Yat-sen University.

H.W. and J.L. contributed equally to the current paper.

APPENDIX: THE LGD INTERACTION ENERGY OF POLARIZATION USED IN STOCHASTIC PHASE FIELD MODEL AND THE SIMULATION DETAILS

In SPFM, the LGD free energy is adopted to describe the interaction potential between the polar elements, i.e., $\mathcal{U}$ in the many-body Hamiltonian $\mathcal{H}$ of Eq. (8), as

$$\mathcal{U} = \sum_i \Omega f(P_i) = \sum_{n,\alpha} \Omega f(P_{n,\alpha}), \tag{A1}$$

with $\Omega = 64\,\mathrm{nm}^3$ and f as the volumetric density of interaction potential energy as

$$f = f_{\mathrm{Land}} + f_{\mathrm{grad}} + f_{\mathrm{elec}} + f_{\mathrm{elas}}. \tag{A2}$$

Here, f_{Land} is the Landau bulk free energy for each P_n, which is written as the Taylor expansion of $P_{n,\alpha}$ (to simplify the expression, we drop the subscript n in the following),

$$\begin{aligned} f_{\mathrm{Land}} = {} & a_1 \sum_\alpha P_\alpha^2 + a_{11} \sum_\alpha P_\alpha^4 + a_{12} \sum_{\alpha>\beta} P_\alpha^2 P_\beta^2 \\ & + a_{111} \sum_\alpha P_\alpha^6 + a_{112} \sum_{\alpha\neq\beta} P_\alpha^4 P_\beta^2 \\ & + a_{123} \prod_\alpha P_\alpha^2 + a_{1111} \sum_\alpha P_\alpha^8 \\ & + a_{1112} \sum_{\alpha\neq\beta} P_\alpha^6 P_\beta^2 + a_{1122} \sum_{\alpha>\beta} P_\alpha^4 P_\beta^4 \\ & + a_{1123} \sum_\alpha P_\alpha^2 \prod_\beta P_\beta^2, \end{aligned} \tag{A3}$$

where $\alpha, \beta = x, y, z$, and all the $\boldsymbol{a}$ are the expansion parameters, whose values are listed in Table I, and also can be referenced in Ref. [18]. f_{grad} is the gradient term,

$$f_{\mathrm{grad}} = \sum_{\alpha,\beta} \frac{G_l}{2} \left(\frac{\partial P_{n,\alpha}}{\partial r_\beta} \right)^2, \tag{A4}$$

where $G_l = G_1$ if $\alpha = \beta$ and $G_l = G_2$ if $\alpha \neq \beta$, with G_1 and G_2 being the gradient coefficients, whose values are listed in Table I. f_{elec} is the electrostatic term as

TABLE I. Parameters used in SPFM simulations for polarization switching of BaTiO$_3$, from Ref. [18].

Parameter	Value
a_1	$(T - 388) \times 4.124 \times 10^5$ [JmC^{-2}]
a_{11}	-2.097×10^8 [Jm^{5}C^{-4}]
a_{12}	7.974×10^8 [Jm^{5}C^{-4}]
a_{111}	1.294×10^9 [Jm^{9}C^{-6}]
a_{112}	-1.950×10^9 [Jm^{9}C^{-6}]
a_{123}	-2.500×10^9 [Jm^{9}C^{-6}]
a_{1111}	3.863×10^{10} [Jm^{13}C^{-8}]
a_{1112}	2.529×10^{10} [Jm^{13}C^{-8}]
a_{1122}	1.637×10^{10} [Jm^{13}C^{-8}]
a_{1123}	1.367×10^{10} [Jm^{13}C^{-8}]
G_1	4.4539×10^{-11} [Jm^{3}C^{-2}]
G_2	2.2270×10^{-11} [Jm^{3}C^{-2}]
ϵ_b	4.4271×10^{-11} [J^{-1}m^{-1}C^2]
C_{11}	19.8×10^{10} [Jm^{-3}]
C_{12}	9.60×10^{10} [Jm^{-3}]
C_{44}	12.2×10^{10} [Jm^{-3}]
Q_{11}	1.104×10^{-1} [m^{4}C^{-2}]
Q_{12}	-4.520×10^{-2} [m^{4}C^{-2}]
Q_{44}	2.950×10^{-2} [m^{4}C^{-2}]
μ	3.2×10^{-40} [Jm^{4}C^{-2}s^2]
$\gamma = \mu/\tau$	

$$f_{\mathrm{elec}} = -\boldsymbol{P} \cdot \boldsymbol{E} - \tfrac{1}{2} \epsilon_b \boldsymbol{E}^2, \tag{A5}$$

where $\boldsymbol{E}$ is the total electrostatic field, including the external electric field $\boldsymbol{E}_{\mathrm{ext}}$ and depolarization field $\boldsymbol{E}_d$, as $\boldsymbol{E} = \boldsymbol{E}_{\mathrm{ext}} + \boldsymbol{E}_d$; ϵ_b is the background dielectric permittivity. f_{elas} is the electrostrictive term

$$f_{\mathrm{elas}} = \sum_{\alpha\beta\lambda\nu} \frac{1}{2} C_{\alpha\beta\lambda\nu} \left(e_{\alpha\beta} - e^0_{\alpha\beta} \right) \left(e_{\lambda\nu} - e^0_{\lambda\nu} \right), \tag{A6}$$

where $C_{\alpha\beta\lambda\nu}$ are elastic stiffness coefficients, $e_{\alpha\beta}$ are eigenstrain components of the strain tensor $\mathbf{e}$, and $e^0_{\alpha\beta}$ is the eigenstrain induced by the electromechanical coupling, depending on the spontaneous polarization as $e^0_{\alpha\beta} = \sum_{\lambda\nu} Q_{\alpha\beta\lambda\nu} P_\lambda P_\nu$ with $Q_{\alpha\beta\lambda\nu}$ being the electrostrictive coefficients. The values of $C_{\alpha\beta\lambda\nu}$ and $Q_{\alpha\beta\lambda\nu}$ are listed in Table I.

In our SPFM simulations for all the polarization switching processes performed in the main text, the simulation system is discretized into $64h \times 64h \times 64h$ grids with $h = 4.0$ [nm], which is embedded in the heat bath denoted by $T = 300$ [K]. The phase-space trajectories $\{P_i(t)\}$ are obtained by solving the Langevin equation of Eq. (9) derived from the Hamiltonian $\mathcal{H}$ of Eq. (8), where all the parameters are listed in Table I. The Langevin equation is solved via an explicit Euler method with a time step of 1 [fs], and the FFT approach is adopted to calculate the conservative force. The total polarization $P(t)$ of the systems considered is thus thermodynamic observable as $P(t) = \langle P_i(t) \rangle$. The polarization temperature T_P links to the *kinetic energy* as $k_{\mathrm{B}} T_P(t) = \langle \mu \dot{P}_i^2(t) \rangle$, with k_{B} as the Boltzmann constant. Doubling the numbers of meshing grids and decreasing the time step are examined to result in a statistical error less than $\sim$0.1%. The FFT simulations are performed by a self-developed C language code, with the use of the C subroutine library FFTW for computing the discrete Fourier transform and the standard software library CLAPACK for numerical linear algebra.

[1] T. Qi, Y.-H. Shin, K.-L. Yeh, K. A. Nelson, and A. M. Rappe, Collective coherent control: Synchronization of polarization in ferroelectric $PbTiO_3$ by shaped THz fields, Phys. Rev. Lett. **102**, 247603 (2009).

[2] Y. Zheng and W. J. Chen, Characteristics and controllability of vortices in ferromagnetics, ferroelectrics, and multiferroics, Rep. Prog. Phys. **80**, 086501 (2017).

[3] R. Mankowsky, A. von Hoegen, M. Först, and A. Cavalleri, Ultrafast reversal of the ferroelectric polarization, Phys. Rev. Lett. **118**, 197601 (2017).

[4] Z. Gu, S. Pandya, A. Samanta, S. Liu, G. Xiao, C. J. Meyers, A. R. Damodaran, H. Barak, A. Dasgupta, S. Saremi, A. Polemi, L. Wu, A. A. Podpirka, A. Will-Cole, C. J. Hawley, P. K. Davies, R. A. York, I. Grinberg, L. W. Martin, and J. E. Spanier, Resonant domain-wall-enhanced tunable microwave ferroelectrics, Nature (London) **560**, 622 (2018).

[5] J. Liu, Y. Ji, S. Yuan, L. Ding, W. Chen, and Y. Zheng, Controlling polar-toroidal multi-order states in twisted ferroelectric nanowires, npj Comput. Mater. **4**, 78 (2018).

[6] C. Paillard, E. Torun, L. Wirtz, J. Íñiguez, and L. Bellaiche, Photoinduced phase transitions in ferroelectrics, Phys. Rev. Lett. **123**, 087601 (2019).

[7] M. Vopsaroiu, J. Blackburn, M. G. Cain, and P. M. Weaver, Thermally activated switching kinetics in second-order phase transition ferroelectrics, Phys. Rev. B **82**, 024109 (2010).

[8] J. Liu, H. Wen, W. Chen, and Y. Zheng, Atomistic studies of temporal characteristics of polarization relaxation in ferroelectrics, Phys. Rev. B **103**, 014308 (2021).

[9] J. F. Scott, A review of ferroelectric switching, Ferroelectrics **503**, 117 (2016).

[10] W. J. Merz, Domain formation and domain wall motions in ferroelectric $BaTiO_3$ single crystals, Phys. Rev. **95**, 690 (1954).

[11] Y. Ishibashi and Y. Takagi, Note on ferroelectric domain switching, J. Phys. Soc. Jpn. **31**, 506 (1971).

[12] X. Du and I.-W. Chen, Fatigue of $Pb(Zr_{0.53}Ti_{0.47})O_3$ ferroelectric thin films, J. Appl. Phys. **83**, 7789 (1998); A Lorentz field theory for ferroelectric transitions in layered perovskites, Ferroelectrics **208-209**, 237 (1998); Model experiments on fatigue of $Pb(Zr_{0.53}Ti_{0.47})O_3$ ferroelectric thin films, Appl. Phys. Lett. **72**, 1923 (1998).

[13] M. J. Highland, T. T. Fister, M.-I. Richard, D. D. Fong, P. H. Fuoss, C. Thompson, J. A. Eastman, S. K. Streiffer, and G. B. Stephenson, Polarization switching without domain formation at the intrinsic coercive field in ultrathin ferroelectric $PbTiO_3$, Phys. Rev. Lett. **105**, 167601 (2010).

[14] D. Viehland and Y.-H. Chen, Random-field model for ferroelectric domain dynamics and polarization reversal, J. Appl. Phys. **88**, 6696 (2000).

[15] A. K. Tagantsev, I. Stolichnov, N. Setter, J. S. Cross, and M. Tsukada, Non-Kolmogorov-Avrami switching kinetics in ferroelectric thin films, Phys. Rev. B **66**, 214109 (2002).

[16] R. Gaynutdinov, M. Minnekaev, S. Mitko, A. Tolstikhina, A. Zenkevich, S. Ducharme, and V. Fridkin, Polarization switching kinetics in ultrathin ferroelectric barium titanate film, Physica B: Condens. Matter **424**, 8 (2013).

[17] P. Ghosez and J. Junquera, Modeling of ferroelectric oxide perovskites: From first to second principles, Annu. Rev. Condens. Matter Phys. **13**, 325 (2022).

[18] H. Wen, J. Liu, W. Chen, W. Xiong, and Y. Zheng, Thermodynamics of polarization dynamics in ferroelectrics implemented by the phase field model, Phys. Rev. B **106**, 024111 (2022).

[19] J.-J. Wang, B. Wang, and L.-Q. Chen, Understanding, predicting, and designing ferroelectric domain structures and switching guided by the phase-field method, Annu. Rev. Mater. Res. **49**, 127 (2019).

[20] K. Tani, Dynamics of displacive-type ferroelectrics soft modes, J. Phys. Soc. Jpn. **26**, 93 (1969).

[21] H. A. Kramers, Brownian motion in a field of force and the diffusion model of chemical reactions, Physica **7**, 284 (1940).

[22] M. von Smoluchowski, On the kinetic theory of the Brownian molecular motion and of suspensions, Ann. Phys. **326**, 756 (1906).

[23] L.-Q. Chen, Phase-field method of phase transitions/domain structures in ferroelectric thin films: A review, J. Am. Ceram. Soc. **91**, 1835 (2008).

[24] S. Boyn, J. Grollier, G. Lecerf, B. Xu, N. Locatelli, S. Fusil, S. Girod, C. Carrétéro, K. Garcia, S. Xavier, J. Tomas, L. Bellaiche, M. Bibes, A. Barth'l'my, S. Saïghi, and V. Garcia, Learning through ferroelectric domain dynamics in solid-state synapses, Nat. Commun. **8**, 14736 (2017).

[25] J. Rolland, F. Bouchet, and E. Simonnet, Computing transition rates for the 1-D stochastic Ginzburg-Landau-Allen-Cahn equation for finite-amplitude noise with a rare event algorithm, J. Stat. Phys. **162**, 277 (2016).

[26] B. Xu, V. Garcia, S. Fusil, M. Bibes, and L. Bellaiche, Intrinsic polarization switching mechanisms in $BiFeO_3$, Phys. Rev. B **95**, 104104 (2017).

[27] A. K. Tagantsev, L. E. Cross, and J. Fousek, *Domains in Ferroic Crystals and Thin Films* (Springer, New York, 2010).

[28] G. Gerra, A. K. Tagantsev, and N. Setter, Surface-stimulated nucleation of reverse domains in ferroelectrics, Phys. Rev. Lett. **94**, 107602 (2005).

[29] K. Ito, On stochastic differential equations, Am. Math. Soc. **4**, 1 (1951).